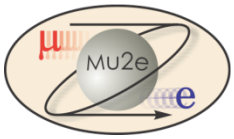

Fermilab

Requirements for the Mu2e Production Solenoid Heat and Radiation Shield

V15

G. Ambrosio, R. Coleman, V. Kashikhin, M. Lamm, M. Lopes,
N. Mokhov, J. Popp, V. Pronskikh

Mu2e-doc-1092
5/5/2014

Requirements for the Mu2e Production Solenoid Heat and Radiation Shield

This document describes the Heat and Radiation Shield (HRS). The HRS serves to protect the superconducting coils of the Production Solenoid (PS) from the intense radiation generated by the 8 GeV kinetic energy primary proton beam striking the production target within the warm bore of the PS. This shield also protects the coils in the far upstream end of the Transport Solenoid (TS), a straight section of coils called TS1, at the exit from the PS. The HRS aperture should allow the maximum stopping rate of negative muons in the Detector Solenoid stopping target.

There are a number of requirements for the HRS:

1. Production Solenoid Heat and Radiation

   a) Limit the continuous power delivered to the cold mass

   b) Limit the local heat load allowed anywhere within the superconducting coils

   c) Limit the maximum local radiation dose to the insulation over the lifetime of the experiment

   d) Limit the damage to the cable aluminum stabilizer and copper matrix

2. Production Solenoid field quality should not be degraded by materials used in the HRS

3. Production Solenoid forces during a quench should be minimized by the choice of HRS materials, if possible. The HRS electrical resistivity must be high to limit forces from eddy currents during a quench.

4. Transport Solenoid Heat and Radiation (see #1 above)

5. HRS thermal cooling system should limit the temperature on the surface of HRS. The inner surface holds the target support. The outer surface is adjacent to the PS cryostat and in contact in a few locations.

6. Muon Yield should not be reduced significantly by the inner bore size of the HRS.

7. In addition, an acceptable shield design must avoid any line-of-sight cracks between components that point from the target to the inner cryostat wall and thus the magnet coils.

8. To insure a good lifetime for the radiatively cooled production target, a vacuum level of 1 x 10-5 torr is required. Materials used in the HRS should not limit this vacuum level.

1. Production Solenoid Heat and Radiation

a) Limit the continuous power delivered to the cold mass

An acceptable shield design should establish the following quench limits for nominal operating conditions with the proton beam striking the target: the maximum allowable total heat load for the PS cold mass is 100 W [1].

b) Limit the instantaneous local heat load allowed anywhere within the superconducting coils

A current thermal analysis [1] suggests that the maximum tolerable local heat deposition in the superconductor is 30 μW/g.

c) Limit the maximum local radiation dose to the coil insulation and epoxy over the lifetime of the experiment

In principle, each material included in the construction of the magnet should be rated for the maximum allowable local radiation dose over the operational lifetime of the experiment. In practice, the most radiation-sensitive material sets the lower limit; in particular, the epoxy used to bond the insulation to the superconducting cable can tolerate a maximum of 7 MGy before it experiences a 10% degradation in its shear modulus. The figure below shows some measurements of epoxy damage [2].

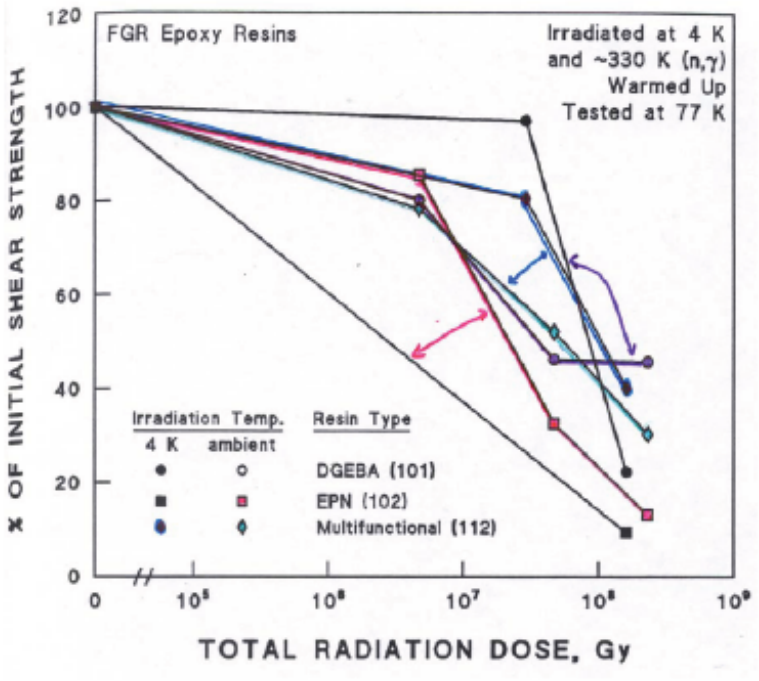

Figure 1.25. A comparison of the shear strengths of three types of reinforced epoxy resins that were reactor-irradiated at both 4 K and at ambient temperature. See text for differences in the fast neutron spectrum in the two reactors. Data from Munshi [1991]. (Supplementary Tables A. 3-3 and A. 8-4.)

Fig 1 Epoxy Radiation Damage

d) Limit the damage to the cable's Aluminum stabilizer and Copper Matrix

Introduction

The final parameter describes how radiation affects the electrical conductivity of the component metals of the superconductor cable. At liquid helium temperature, damage to the atomic lattice of a superconducting cable and its quench-stabilizing matrix made from normal conductor takes the form of the accumulation of atomic displacements; i.e., tiny lattice defects. After exposing a metal sample to a given neutron flux spectrum the damage can be characterized by the average number of displacements per atom (DPA). The DPA is directly related to electron transport in metals. The Residual Resistivity Ratio (RRR) is defined as the ratio of the electrical resistance at room temperature of a conductor to that at 4.5 K. For a given sample exposed to various neutron spectra, the RRR will decrease. However, warming such a sample to room temperature leads to recovery of the RRR [3,4], but the degree of recovery depends on the metal. Aluminum is one example material that shows complete recovery, or nearly so, at 300 K. The annealing time was seen to be on a time scale of minutes [4]. This is to be compared to the PS during warm-up or cool-down times; each would be of order days.

The effect of RRR on the magnet performance

RRR is an important parameter for the superconducting magnet design that affects the magnet performance during operation in superconducting mode and irreversible transition to the normal state (quench). The following list summarizes the most important areas of the magnet performance affected by the RRR:

- *Magnet stability* is the ability of coils to recover the superconducting state after a brief transition into the normal state without the quench. The superconductor transition to the normal state occurs when either the magnetic field, temperature or current exceed the critical values. It can happen for a number of reasons, including rapid heat releases due to cracks in epoxy, slip-stick motion of turns and coils, temperature fluctuation in the cooling system, voltage spikes in the powering circuit and the primary beam mis-steering into the cold mass. While some of the perturbations can be minimized, most cannot be eliminated, and it is therefore safe to assume that a critical perturbation can happen at any given moment during the magnet operation. When it happens, the electric current flowing in the superconductor is forced into the surrounding Cu and Al stabilizers that have much lower resistivity than the superconductor in normal state. The stabilizer resistivity is sufficiently low (i.e. the RRR is sufficiently high) when the resistive heating power of current flowing in the stabilizer is lower than the cooling power due to the heat transfer into the surrounding media. In that case, the temperature returns to the operating temperature after a brief excursion during the critical perturbation. In the opposite case, the normal zone propagates throughout the coil and eventually all turns transit to the normal state that constitutes the quench.
- *Quench protection* is protection of the magnet during quench from overheating and overvoltage. The resistive heating power of current flowing in the stabilizer during quench is proportional to the stabilizer's resistivity. Therefore, the peak coil temperature during quench is directly affected by the RRR. If the RRR is not sufficiently high, the peak temperature can exceed the maximum acceptable value that is chosen to limit the thermal stresses due to the temperature gradient in the coil. In that case, the thermal stresses can cause damage to the cable or ground insulation.
- *Cooling* during normal operation. The particle radiation deposits a considerable amount of heat in the superconducting coils. In order for the magnet to operate reliably, the coil temperature must be kept below the critical value with a sufficient thermal margin. It is achieved by a system of thermal bridges connecting all turns to the cooling system. For structural reasons, the thermal bridges are made from Al with the same chemical composition as the cable stabilizer. Therefore, it is reasonable to assume that the same degree of radiation damage occurs in the thermal bridges as it does in the cable stabilizer. The ability of the thermal bridges to conduct the heat depends on the thermal conductivity that, according to Wiedemann–Franz law, has the same mechanism as the electric resistivity. Thus it is directly affected by the value of RRR.

The final magnet design will be optimized to work with sufficient operating margins at the minimum RRR of 100 for aluminum set forth in the PS Requirements Document [5]. The aluminum RRR will set the limit on DPA. The role of RRR of copper is critical for magnet stability and less important for cooling and quench protection. It would be desirable for the RRR of copper to remain above about 50.

These margins, governed by the practices applicable to the design of superconducting magnets, do not account for the errors in determining DPA and RRR. Therefore, it is important that the HRS design requirement includes an appropriate safety margin in the maximum acceptable value of DPA to account for these errors.

Measurements of RRR degradation of Aluminum with radiation

The COMET group from KEK has begun a series of measurements at the Kyoto University Research Reactor. In 2011 they irradiated a sample of aluminum to a large flux of neutrons at low temperature [6]. The results are shown below for the increase in resistance vs integrated neutron flux.

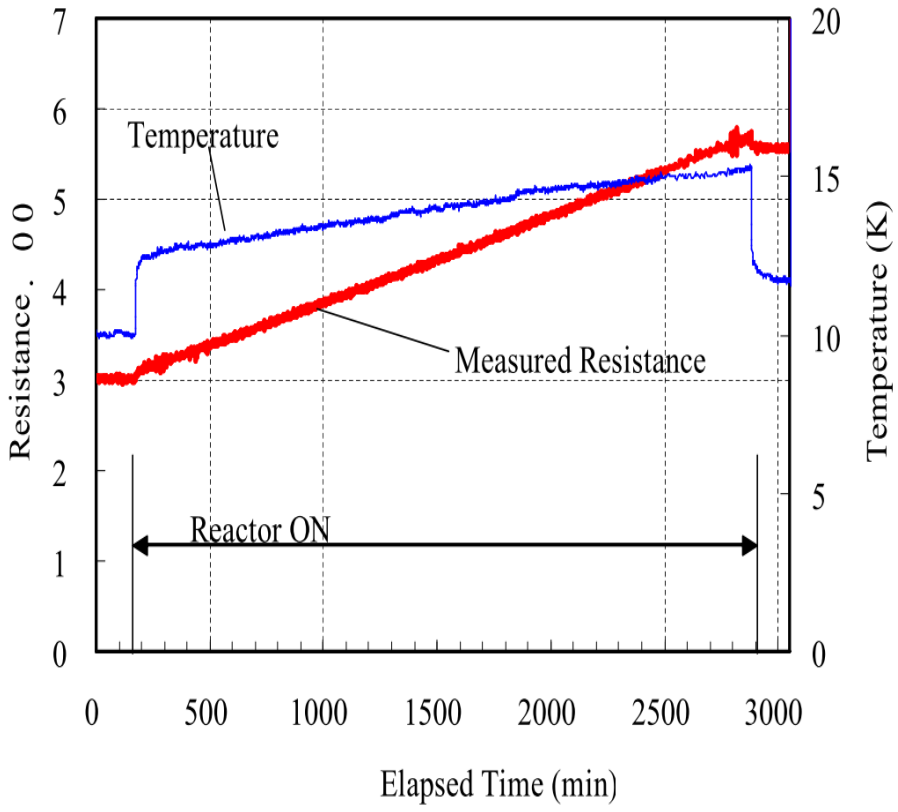

Fig 2 COMET/KEK Measurement

The starting resistance 3.0 μΩ increased to 5.6 μΩ after neutron exposure. The initial resistance before cool down was 1.37 mΩ. The integrated neutron flux is 2.3 E16 neutrons/cm2 [7]. This is the measurement we currently use for the Mu2e projections. Also importantly for Mu2e, this group observed complete recovery of the aluminum samples when the temperature rose to room temperature. This recovery of Al is consistent with prior measurements [3,4].

Some of the other measurements available on aluminum damage from neutron irradiation at 4 K are summarized in the table below. This compilation is taken from Ref [8] that re-analyzes the experiments with modern theory and consistent parameters. The last column shows the overall adjustment (efficiency η) between analyzed measurements and NRT that varies from 0.357 to 0.535. We will use this range to estimate the uncertainty on our DPA calculation.

Table 1 Summary of Measurements

Measurement	Energy [MeV] or Source	Flux {1E16} Per cm2	Δρ [nΩ-cm]	Δρ/Flux [nΩ/cm]	$\langle\sigma T_d\rangle$ [b*keV]	$\eta = N_D/N_{NRT}$
CP-5(VT53) ANL Kirk et al, Horak 1979 [3,12]	fission ~0.1-7.0	200	382	1.5	76.2	0.357
FISS,FRAGM CP-5 ANL Birtcher et al 1977 [12,13]	fission			57.6	2492.	0.422
LTIF, ORNL Coltman,Klabunde 1982 [14,15,16]	fission	12.3		2.19	98.55	0.405
RTNS,LLL Guinan et al 1982 [16]	14-15	8.2	33.6	4.18	156.9	0.486
LHTL,JPR-3 Takamura et al 1985 [17]	fission	4-12		2.2	81.0	0.495
TTB(1),FRM Wallner et al 1987 [18]	reactor	830	798	2.57	87.6	0.535
COMET/KEK Yoshida et al [7,8]	reactor	2.3 >.1 MeV	5.1	2.2		

Fig 3 Neutron Energy Spectrum for Experiments Prior to COMET/KEK

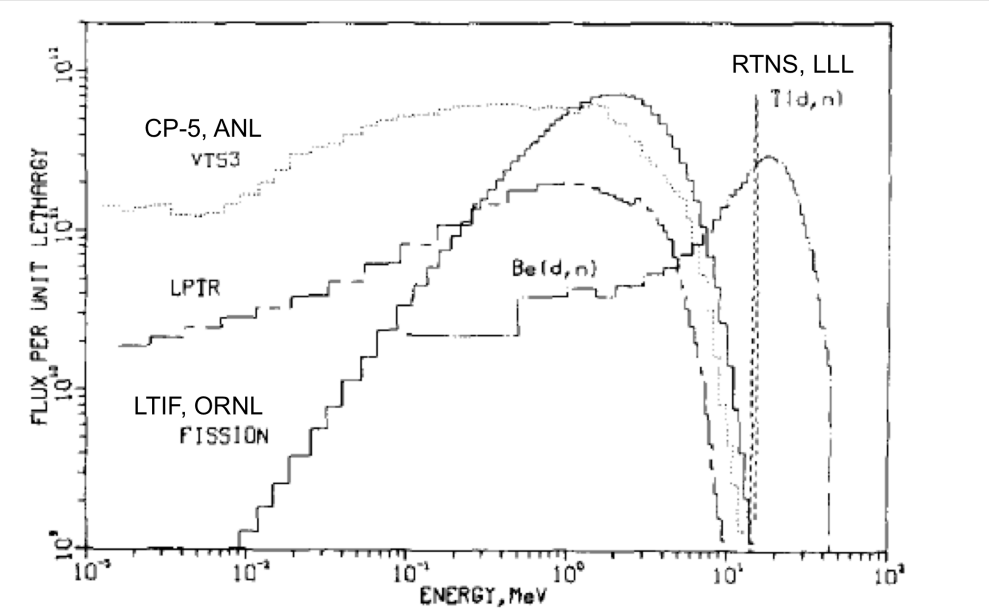

Fig 4 KEK/COMET neutron spectrum compared with other neutron measurements

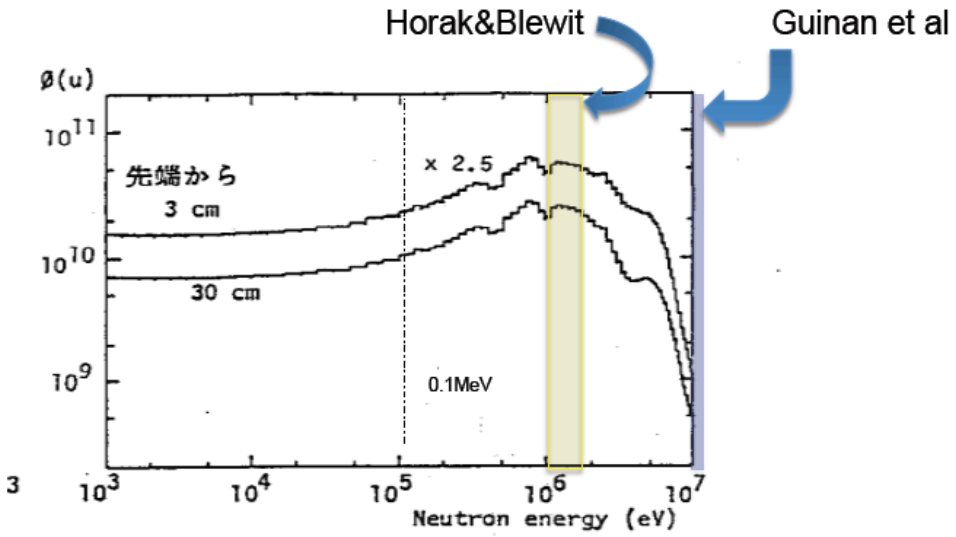

Fig. 15 Neutron energy spectrum in LTL of KUR for ordinary core (above 1000 eV)

KUR-TR287 (1987)

Calculation of DPA for the KEK measurement

Since the KEK measurement was done with a different neutron energy spectrum than Mu2e, a calculation of DPA is needed to relate to Mu2e. The model for DPA uses the cross section shown below vs. neutron energy in eV [9].

Fig 5 DPA cross section vs neutron energy (eV)

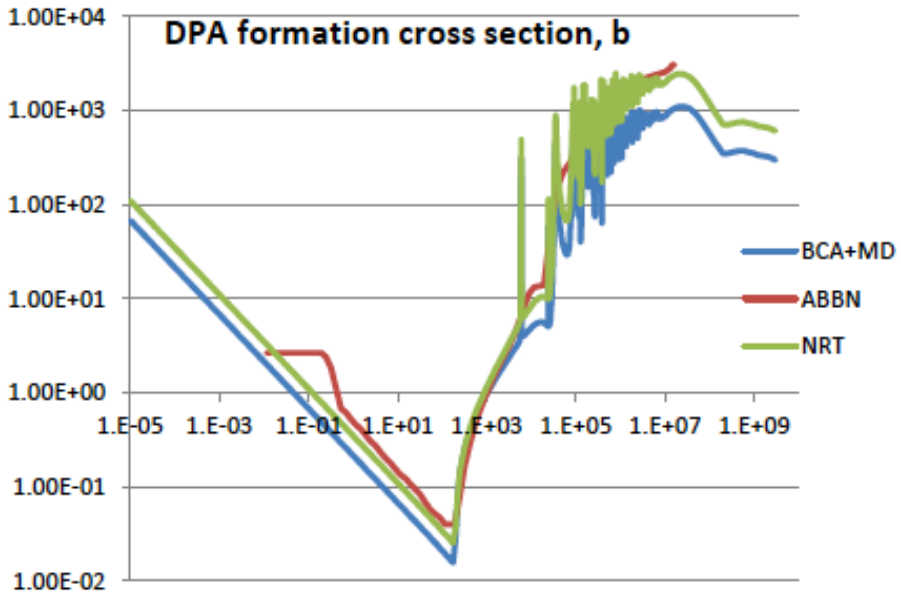

The BCA+MD and NRT models are described in EVAL in Ref [10]. The ABBN model is described in Ref [11].

A comparison of these models with DPA damage from protons on Copper and Tungsten is shown below. While the BCA+MD model agrees better with the data at 1 GeV, in the lower energy region important for Mu2e, the data cannot distinguish the models.

Fig 6 DPA for p + Cu vs Energy

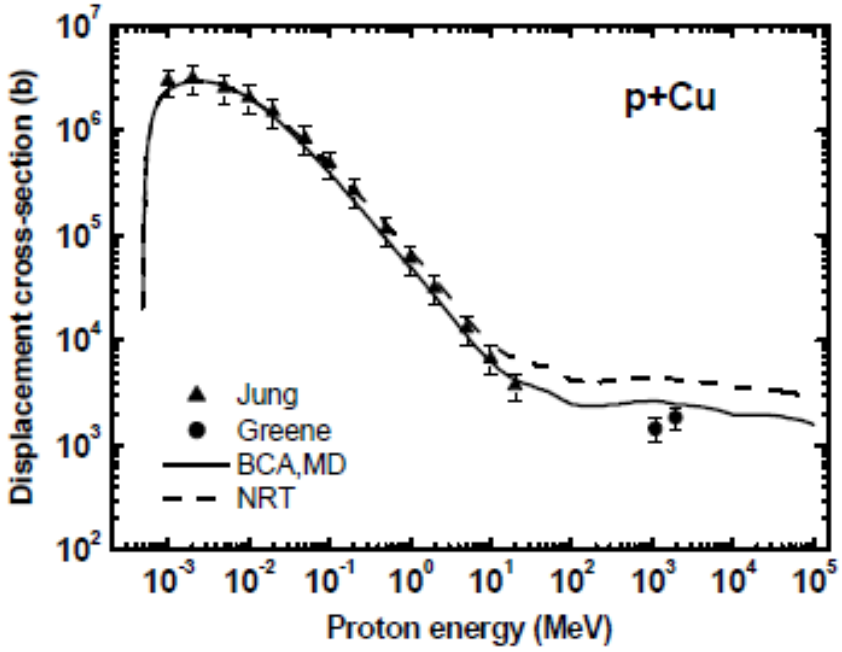

Fig 7 DPA for p+W vs Energy

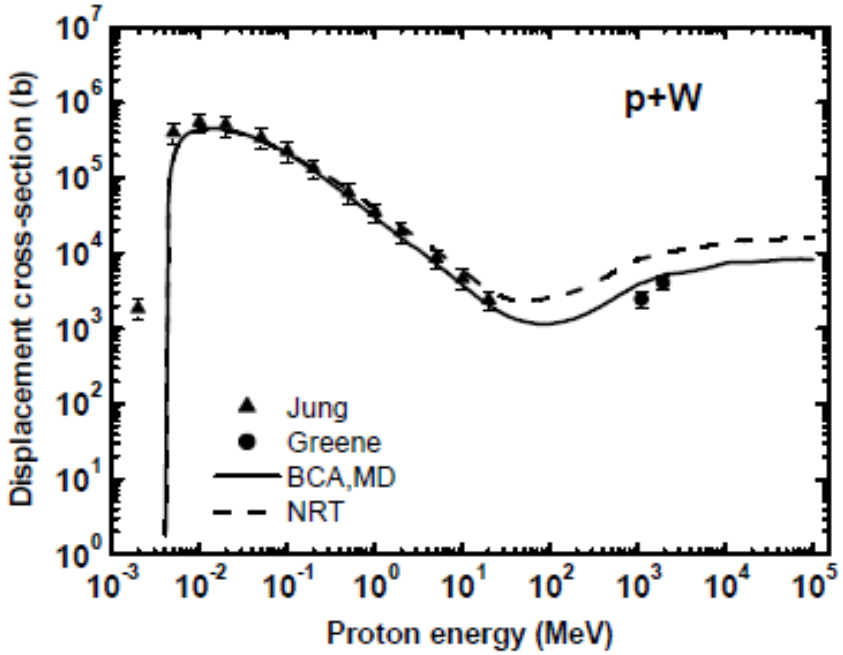

Folding the DPA cross sections with the KEK neutron energy spectrum gives:

Table 2 DPA calculated for KEK measurements

DPA model	DPA
BCA+MD	1.0 E-5
NRT	2.5 E-5
ABBN	2.6 E-5

We can now use the KEK measurement of the change in resistance of the Al sample along with the Mu2e-allowed RRR reduction of 600 to 100, to get limits on DPA exposure for Mu2e. The change in resistivity for the KEK experiment is 5.1 nΩ-cm. Dividing by the DPA in the table above gives the change in resistivity per DPA shown in the table below.

Table 3 Results on DPA for RRR reduction of 600 to 100 for Mu2e

Measurement/DPA model	DPA [E-5]
BCA+MD	4.5
NRT	11
NRT-exp (using average $\eta = N_D/N_{NRT}$)	5.0

Limit on DPA in Aluminum

The KEK data and the DPA calculation for their neutron spectrum are applied to the Mu2e heat shield and neutron spectrum. We find the reduction in the RRR from 600 to 100 would require a DPA of 5×10^{-5} using NRT-exp. This amount is allowed in one year of operation, which would be followed by a warm-up to anneal the aluminum stabilizer. To set a range in the limit, we use the spread in the efficiency $\eta = N_D/N_{NRT} = 0.357$ to 0.535. This gives us a limit of 4 to 6 E-5 for the DPA per year in Mu2e. Fig. 8 below shows the limit along with how RRR varies with DPA.

Fig 8 RRR vs DPA showing a range of DPA of 4 to 6 E-5

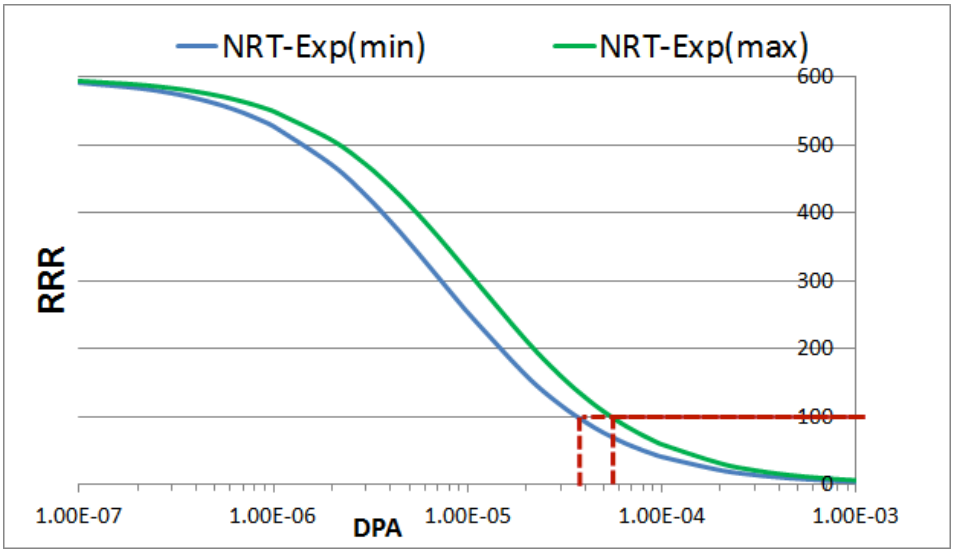

As a check of the DPA calculated using MARS15, 3 different codes were used to compare the calculated DPA. The neutron flux from MARS15 for the highest damage region was input to each of the other 3 codes. A 10 cm thick Al box with a 10x10 cm cross section broken in ten 1 cm thick segments was used to model the coil stabilizer. The region of highest damage is near the proton beam exit end of the HRS. The resulting DPA from the different codes agree to about 15% [19]. The results are shown in Figure 9 below.

Fig 9 DPA for the worst damage region of the Al from 3 simulation codes

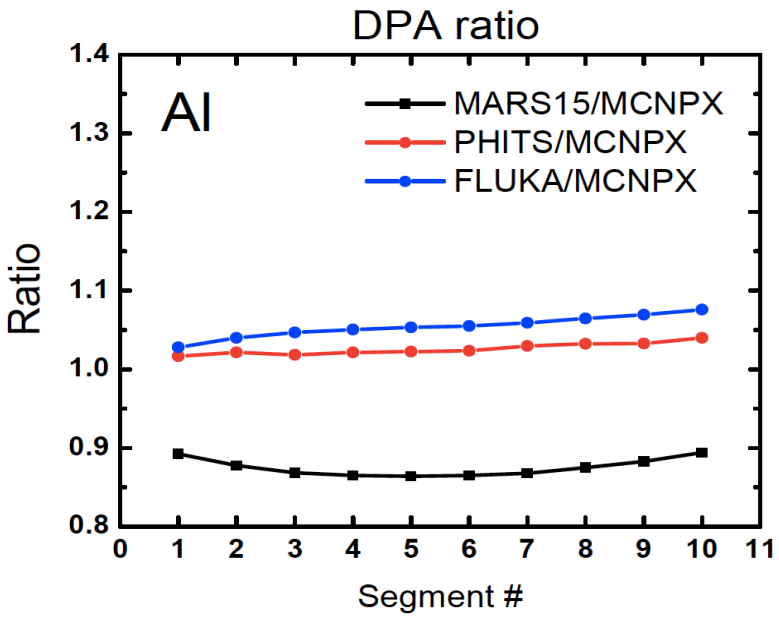

RRR Reduction in Copper

For Copper we use the measurement the change of resistivity with DPA from the COMET group from KEK 2012 measurements at the Kyoto University Research Reactor [20]. Then minimum and maximum ranges are determined as they were for Aluminum using the compilation of measurements from Ref. 8. The results are shown in Fig 10 below. The resulting reduction is RRR of copper to 50 for our DPA limits of 5 to 7 E-5.

Fig 10 Reduction of RRR for Copper

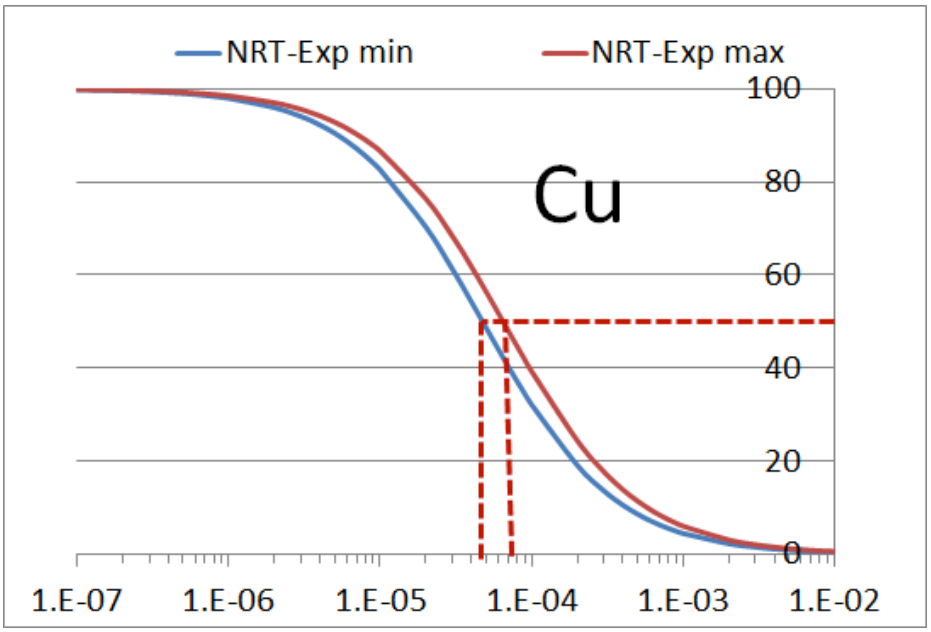

2. Production Solenoid Field Quality

The materials used to construct the shield must not cause the magnetic field to fail to meet the required field quality within tolerances, therefore materials with magnetic permeability <1.10 at the room temperature are required [21].

3. Production Solenoid Forces During a Quench

There can be a large axial force on the coils due to eddy currents in the HRS during a quench. Both the choice of materials and construction of the HRS will determine these forces. Higher resistivity materials can reduce these forces (for example bronze C63200 has ~10x higher resistivity than copper). The choice will depend on the trade-off of HRS material and construction cost vs. additional coil support. The resistivity of selected HRS material shall be $>1\times10^{-7}$ Ω·m at the room temperature [21].

4. Transport Solenoid Heat and Radiation

Power density limits are tighter than PS requirements because the heat extraction from the TS coils is more difficult than from the PS coils (TS has a smaller cable size and more layers without Al-sheets inside the coils). The DPA requirements are also tighter than PS because of the stability requirements due to the larger displacements of TS coils during energization.

Therefore the TS DPA requirement is $< 1.5\ 10^{-5}$ DPA/yr and the power density requirement is <10 μW/g. The total heating should be < 0.5 W in TS1 and TS2 [22].

5. HRS Thermal Cooling system should limit the temperature on the surface of HRS

The HRS water temperature must be greater than 5^0 C to avoid freezing. The outer surface is adjacent to the PS cryostat and in contact in a few locations. The HRS contacts the PS bore at the two end flange weld joints and on the sliding bearing that carries the upstream weight to the PS bore. In the case where the beam is off and the PS is cold, it's very unlikely there would be any danger of the water freezing based on the expected PS inner cryostat temperature (~ 300K). The HRS water temperature will be monitored.

The HRS will include stable mounting features that provide a mechanical connection between the target support structure and inner bore of the HRS vessel. In addition, to avoid overheating of the target support structure, the inner wall of the HRS vessel will be cooled such that its operating temperature stays below 100^oC.

6. Muon Yield should not be reduced significantly by the inner bore size of the HRS.

The inner shield wall is limited to no less than 20 cm [23] since smaller radii negatively impact the stopped muon yield in the Detector Solenoid.

7. In addition, an acceptable shield design must avoid any line-of-sight cracks between components that point from the target to the inner cryostat wall and thus the magnet coils.

Simulations indicated that only cracks larger than a few millimeters are of concern; this should not be a problem.

8. To insure a good lifetime for the radiatively cooled production target, a vacuum level of 1 x 10-5 torr is required.

Outgassing from the inner liner of the HRS should be minimized. The exact requirements await a complete vacuum system specification.

References:

1. Mu2e Conceptual Design Report (chapter 7), March 2012, Mu2e-docdb-1169.
2. Radiation Hard Coils, A. Zeller et al, 2003, http://supercon.lbl.gov/WAAM
3. Isochronal Recovery of Fast Neutron Irradiated Metals, J. Horak and T. Blewitt, J. Nucl. Mat., 49(1973/74) 161-180.
4. Defect Production and Recovery in FCC Metals Irradiated at 4.2 K, M.Guinan et al, J. Nucl. Mater. 133&134 (1985) 357-360.
5. Mu2e Production Solenoid Requirements Document, M. Lamm & V. Kashikhin, April 2011, Mu2e-docdb-1406.
6. COMET Magnets Design and Radiation Effects, M. Yoshida, Mar. 2011, Mu2e-docdb-1406.
7. M. Yoshida et al, ICMC2011.
8. Development of Calculation Methods to Analyze Radiation Damage, Nuclide Production and Energy Deposition in ADS Materials and Nuclear Data Evaluation, C. Broeders and A. Konobeyev, Aug. 2006, Volume 7197 of Wissenschaftliche Berichte // Forschungszentrum Karlsruhe in der Helmholtz-Gemeinschaft
9. DPA Calculation in the Reactor Neutron Energy Range, V. Pronskikh and N. Mokhov, June 2011, Mu2e-docdb-1851.
10. EVAL-Oct 10 by U. Fischer and A.Yu. Konobeyev
11. S. V. Zabrodskaya et al, IPPE, 1993.
12. M.A. Kirk, L.R. Greenwood, J. Nucl. Mater. 80 (1979) 159.
13. R.C. Birtcher, R.S. Averback, T.H. Blewitt, J. Nucl. Mater.75 (1978) 167.
14. R.R. Coltman, Jr., C.E. Klabunde, J.M. Williams, J. Nucl. Mater. 99 (1981) 284.
15. C.E. Klabunde, R.R. Coltman, J. Nucl. Mater. 108&9 (1982) 183.
16. M.W. Guninan, J.H. Kinney, J. Nucl. Mater. 108&9 (1982) 95.
17. S. Takamura, T. Aruga, K. Nakata, J. Nucl. Mater. 136(1985).
18. G. Wallner et al, J. Nucl. Mater. 152 (1988) 146-153.
19. V. Pronskikh, Mu2e radiation simulations: uncertainties and levels, Radiation Effects in Superconducting Magnet Materials, RESMM'13 (2013).
20. M. Yoshida, Neutron Irradiation facilities and recent results, RESMM'13 (2013).
21. Private communication with V. Kashikhin, FNAL.
22. Private communication with G. Ambrosio, FNAL.
23. Mu2e Muon Yield Sensitivity to Production Solenoid Inner Bore Radius, K. Lynch and J. Popp, August 2013, Mu2e-docdb-3226.